Proceedings World Geothermal Congress 2015
Melbourne, Australia, 19-25 April 2015

Surface Movement Induced by a Geothermal Well Doublet

Peter A. Fokker, Ellen F. van der Veer and Jan-Diederik van Wees

TNO, Princetonlaan 6, 3584 CB Utrecht, The Netherlands

peter.fokker@tno.nl; jan_diederik.vanwees@tno.nl

Keywords: subsidence, monitoring, thermo-elasticity

ABSTRACT

We investigated the impact of the exploitation of a typical geothermal well doublet on surface movement and fault (re)activation. When the pressure distribution is stationary, the largest effect should be expected from the progressive cooling of the reservoir, through the thermo-elastic coupling. The absolute value of the expected subsidence is low, but possibly measureable if circumstances are favorite. In that case the distribution of the subsidence can be used to obtain knowledge about the distribution of the cooled part of the reservoir. In addition, the shape of the subsidence pattern obtains information about the subsurface parameters like the elastic profile. In particular when horizontal displacements are available alongside vertical displacement, this information can be used in an inversion exercise to constrain the value of the elastic modulus. A proper monitoring strategy will help to optimize the information to be obtained. Fault reactivation is restricted to the injected temperature front. Stress paths in the fault plane depend on the location on the fault. Inside the reservoir, stress paths are critical and failure can be expected when the temperature front passes the fault. Above and below the reservoir the stress state returns to close-to-initial values when the temperature front has passed and no failure was observed. The risk for inducing seismic events that damage the producing reservoir is very low, although there is a small potential to induce felt events.

1. INTRODUCTION

The exploitation of geothermal heat involves injection and production of cold and hot water, respectively, thus impacting the subsurface conditions. Large amounts of subsidence have been observed in areas where geothermal water or steam have been produced without compensating injection operations. Induced seismicity has also been documented in a number of operating geothermal fields. If injection is performed for pressure maintenance and injection and production rates are equal, the net water extraction rate from the surface vanishes; however the pressure of the water in the reservoir will increase around the injection well and decrease around the production well. This will still have a poro-elastic geomechanical effect: the changed pressures induce stress changes, associated decompaction and compaction around the injector and producer and can potentially cause fault (re)activation. Once the equilibrium has been established, the geomechanical response due to pressure changes will also have stabilized. This is different from the thermoelastic effect due to cooling. For geothermal heat production using a well doublet, there is an ongoing extraction of heat from the subsurface: the area where the formation temperature around the injection well has been decreased will continue to grow during operation of the field. Through the thermo-elastic effect, this cooling will result in ongoing compaction and associated subsidence of the surface; it may also trigger fault movement.

We have quantified the surface movement and the potential for fault reactivation to be expected for a representative geothermal field in the Netherlands. Thereby, we made a first-order approximation of associated seismic magnitudes. We have chosen the Netherlands setting as it is exemplary for direct heat production from mature oil and gas sedimentary basins (e.g. Kramers et al., 2012). Hot water is extracted from clastic aquifers from 1500-3000 m depth which have been explored for oil and gas production in the past (Fig. 1). In such an environment geothermal development benefits considerably from (public) availability of data and models of the subsurface. Furthermore, the Netherlands is marked by an excellent match between heat demand (of greenhouses) and subsurface potential. Consequently, geothermal energy in the Netherlands has been growing rapidly over the last decade, resulting in 8 operational systems and more than 50 being explored. Over 14 litho-stratigraphic units (clastic aquifers) are potential targets for geothermal reservoir development, providing suitable temperatures for direct heating, economic depths, and excellent transmisivity to produce the heat with limited pumping pressures (Pluymaekers et al., 2012; Van Wees et al., 2012).

With the advent of operational doublets and many more being developed, there is a raising concern about potentially harmful effects of subsidence and induced seismic events. The Dutch environment is sensitive to it, being located largely below sealevel and densely populated. For gas reservoirs, subsidence is routinely estimated prior to production and monitored during production. Models and data show over 30cm of subsidence in some cases (de Waal et al, 2012). According to the Dutch mining act special monitoring and mitigating measures are required if anticipated subsidence is substantial (>5 cm). In ongoing and planned geothermal projects in the Netherlands, subsidence is generally expected to be minor as aquifer pressure balance is maintained. However the effects of cooling have sofar not be evaluated. Besides subsidence, ongoing induced seismic events in the northern part of the Netherlands, have recently raised concerns about the effects of gas production in this area due to damage to local urban building. This paper sheds light on the potential effect of subsidence and fault (re)activation in geothermal doublets in clastic aquifer settings. The effect of subsidence was determined through a numerical modelling study for representative aquifer geometries and production rates, by assessing the combined effect of the pressure change around the injection and production well, and of the cooling around the injection well. Fault reactivation was analyzed through analytical methods by determination of the thermo-elastic stress change on a fault plane and estimation of associated earthquake magnitudes.

2. RESERVOIR MODEL

We formulated our reference case to be typical for many Netherlands greenhouse farmers who are using geothermal heat directly for their operations (Van Wees et al, 2012). The case employs a field at 2 km depth, equipped with a production well and an injection well at 1.5 km distance. The thickness of the reservoir was chosen to be 100 m. Injection and production were both set at 200 m^3/hr. Equal injection and production rates ensured a constant amount of water in the reservoir pore volume and no change in the average reservoir pressure. Once operations had started, the pressures remained roughly constant. The injected water had a temperature of 30°C; the original reservoir temperature was 85°C. As a consequence, the reservoir around the injection well was gradually cooled down. We proceeded our calculations until 100 years after starting the injection. This corresponded to a total amount of injected water of about 175 million m^3.

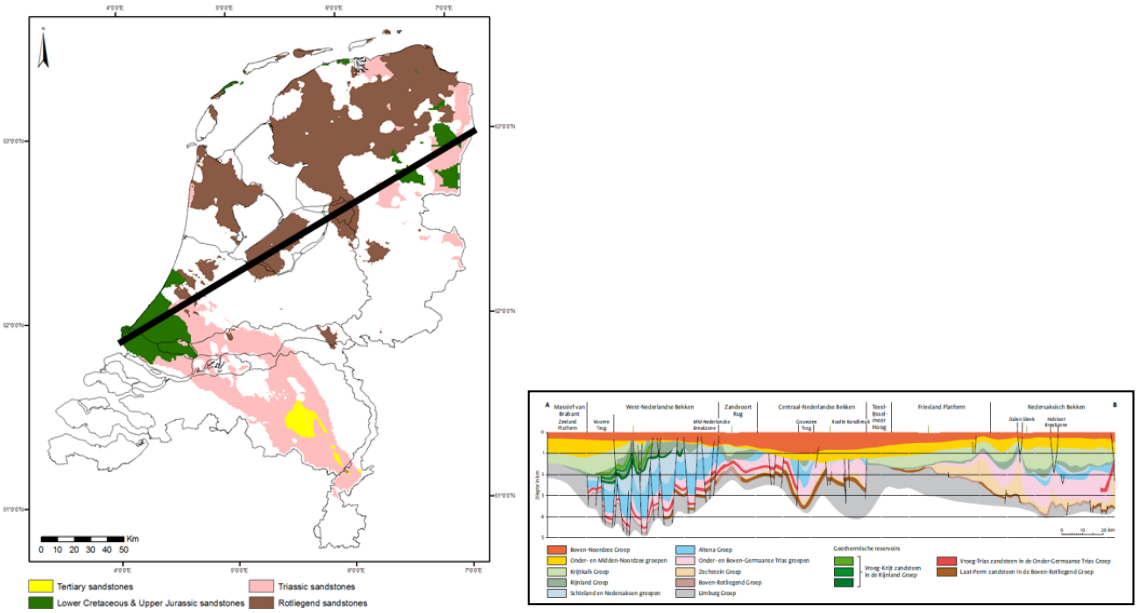

Figure 1: aquifers targeted for geothermal energy production in the Netherlands. (left) subsurface clastic aquifer potential classified in 4 stratigraphic units, (right) NW-SE cross section, highlighting map view potential corresponding to depth of reservoirs of 1500-3000m, and typical thickness ranging from 10s to 200m

To calculate the pressures in the reservoir we employed a numerical steady-state solution adopting a volume-centered 2D finite-difference scheme for the constitutive equation of Darcy flow. The permeability was assumed to be homogeneous with a value of 200 mD. The water viscosity was dependent on the pressure and the temperature following Van Wees et al. (2012), in the reservoir corresponding to ca 0.46 and 0.96 mPa.s for 85°C and 30°C respectively. The reservoir porosity was chosen 20%.

The temperature evolution was calculated by a transient explicit finite difference solution for the heat equation, dedicated for taking into account heat advection and thermal diffusion (cf Van Wees et al., 1992). For the temperature development we assumed direct thermal exchange between the water and the formation. For the thermal advection we adopted fluid velocities from the pressure solution, updated at yearly intervals as a function of changes in the spatial distribution of the viscosity. The thermal advection resulted in a rather sharp temperature front travelling from the injection well into the reservoir; inside the front the temperature was 30°C, outside it was 85°C. Input values for the heat balance were the density and heat capacity of the water and rock matrix. The first is temperature, density and salinity dependent (cf Van Wees et al., 2012), adopting a salinity of 70,000 ppm. For the density and heat capacity of the rock matrix, values of 2700 kg/m^3 and 1000 J/[kg K] were used.

Coupling of the pressures and temperatures to the mechanic behaviour of the subsurface is through poro-elasticity and thermo-elasticity. A pressure increase will cause the reservoir expansion; a temperature decrease will cause shrinkage. A quantitative geomechanical treatment needs to consider the complete subsurface because the complete subsurface is connected geometrically. Furthermore, the coupling is in principle a two-way coupling: the pore volume will change as a result of geomechanical volume strain. For the present investigation we only considered a one-way coupling in which the changed pressure and temperature fields influence the stresses and displacements. This allows the use of the pressure and temperature fields as input in a geomechanical code and to run the codes sequentially. For the geomechanics we used the semi-analytical approach of Fokker and Orlic (2006). The semi-analytic nature of the algorithm makes the approach very fast, while still some basic geologic features like a layering of the subsurface can be taken into account. Another possible approach is Geertsma's analytical model for fully homogeneous subsurface (1970). Both models can account for the areal distribution of the driving forces through the employment of an influence function that is applied on each grid point in the reservoir where compaction takes place. The combined influence of the field is calculated by superposition of the influence of all reservoir gridblocks, which is warranted through the linear character of the geomechanical theory employed. The alternative would be to use a numerical approach with finite elements. Finite elements allow the full modeling of the geological detail, the employment of non-linear models, and can be iteratively coupled to the modelling of the temperature and pressure fields – however for our current application this was considered unnecessary.

We determined the potential for fault movement using 3D Mohr-Coulomb analysis focusing on the effect of cooling. Induced stress changes were obtained using an analytical thermo-elastic model of a radial-symmetric, isotropic reservoir. The equations describing the thermo-elastic stress changes due to fluid injection were based on the work of Myklestad [1942]. This model allowed for quick calculation of the induced stress change at any point of a pre-defined fault plane, depending on the distance and orientation with respect to the axi-symmetric temperature front. Figure 2 shows the set-up of the model geometry. The temperature difference between the injected water and reservoir rocks was described by a step function.

Seismic magnitudes were estimated using simple seismic relations, assuming that magnitude is dependent on stress drop and the fault's areal extend [Aki 1972].

As input for the geomechanical calculations we had a poroelastic compaction coefficient of $1*10^{-5}$ bar^{-1} and a thermoelastic expansion constant of $2*10^{-5}$ K^{-1}. The elastic moduli in the reservoir were chosen as E = 9 GPa and $\nu = 0.35$.

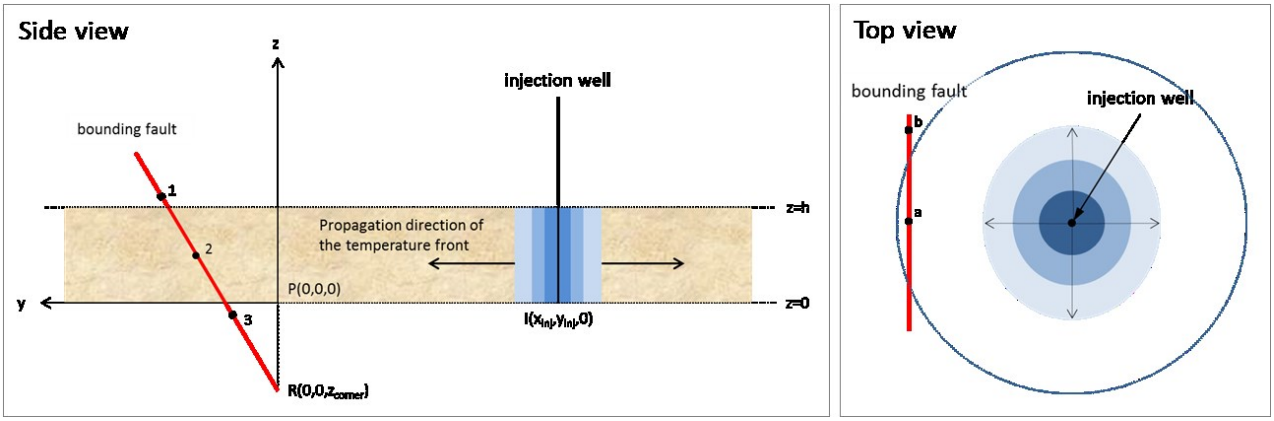

Figure 2 Geometry set-up for the radial symmetric, analytical thermo-elastic model. Left: Side view. Right: Top view. The injected cold fluid forms a cylinder around the injection well and propagates towards the fault due to constant injection. The temperature difference between the injected fluid and the reservoir is described by a step function at the boundary of the cylinder. The fault is permeable and so forms no barrier to the approaching temperature front. Note that the temperature front is linked to but different from the fluid front, as the water transfers heat to the reservoir rock. We assumed a normal stress regime with isotropic horizontal stresses, based on typical stress gradients in the Dutch crust. The failure envelope was based on a internal friction coefficient of 0.6. The numbers 1-3 and letters a-b indicate the locations where we determined the stress path for varying along-dip and along-strike directions, respectively.

3. RESULTS

For the representative field case indicated above, we calculated the development of pressures and temperatures. The compaction field, required as input for the geomechanical calculations, was determined from the combined effect of pressure and temperature. An impression of the results is given in Fig.3. The progressive cooling around the injection well is shown by the compaction curves moving outward from the injection well. The maximum amount of compaction is about 10 cm. The effect of constant pressure increase around the injection well (at X = 1750 m) is clear from the slightly smaller compaction around it. The elevated pressure in that region partly compensates the shrinkage by the cooling. Conversely, around the production well (at X = 3250 m) some compaction results from the drawdown applied to the reservoir increase. In absolute values, the pressure effect amounts to no more than 10% of the effect of temperature for the parameters used in this study and they result in a correction of 1 cm at maximum, in a small region around the wells. As stated earlier, this result is critically dependent on the operational choice to balance injection and production rates.

The 2D areal compaction profiles were input in the geomechanical simulator using two different scenarios. The first scenario was with an elastically homogeneous subsurface as used by Geertsma (1973), the second with an elastic profile with increasing Young's modulus with depth to represent a typical stiffening of the subsurface with depth. This stiffening profile is represented in Fig. 4 (left). The resulting horizontal and vertical displacements for a unit volume of compaction at the depth of the reservoir are also indicate in Fig. 4. With an increasing Young's modulus with depth, the subsidence profile is deeper and narrower.

The profiles determined for a unit volume of compaction as represented in Fig. 4 (right) were used as influence function and integrated in the standard manner (Fokker & Orlic, 2006), to obtain areal subsidence patterns. An example is given in Fig. 5 (left). The temporal development of the largest value of subsidence is also represented in Fig. 5 (right). As expected from the influence function (Fig. 4, right), the subsidence is larger for the profile with increasing modulus.

It has been previously shown that the subsidence profile can be used to provide information about the subsurface parameters. This method is even more powerful when vertical as well as horizontal displacements are available (Fokker et al, 2013). Therefore we represented in Fig. 6 the vertical displacements and the horizontal displacements in the x-direction along a line above the injection and production wells. The figure shows that the surface movement is larger for the case with the increasing modulus, but also that the shape is different. For the case with increasing modulus, the gradients are larger, and consequently the horizontal movements are larger with respect to the vertical movements.

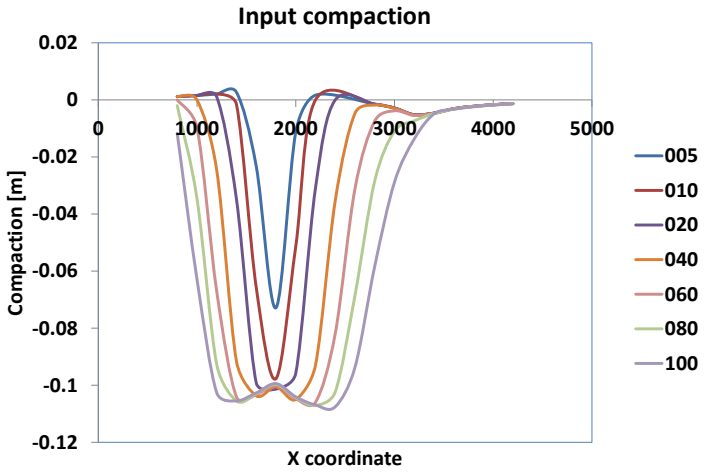

Figure 3 Compaction profile along a line passing injection and production well at 100 m distance. The injection well is at x = 1750 m; the production well at x = 3250 m. Legend indicates time in years.

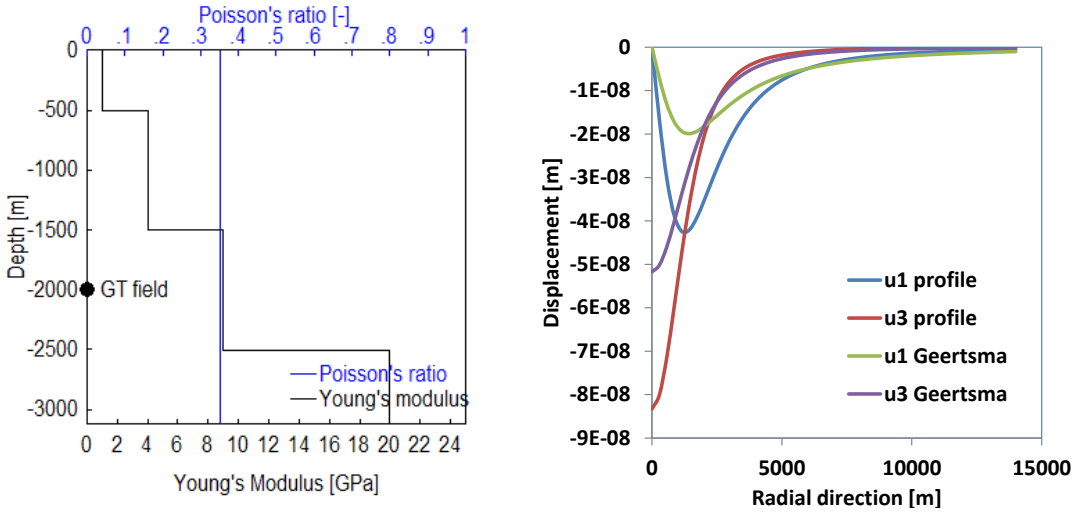

Figure 4 Left: Elasticity profile for the non-homogeneous case. Right: horizontal (u_1) and vertical (u_3) displacement for a unit volume of compaction at 200 m depth; for a homogeneous subsurface (Geertsma) and for the profile represented left.

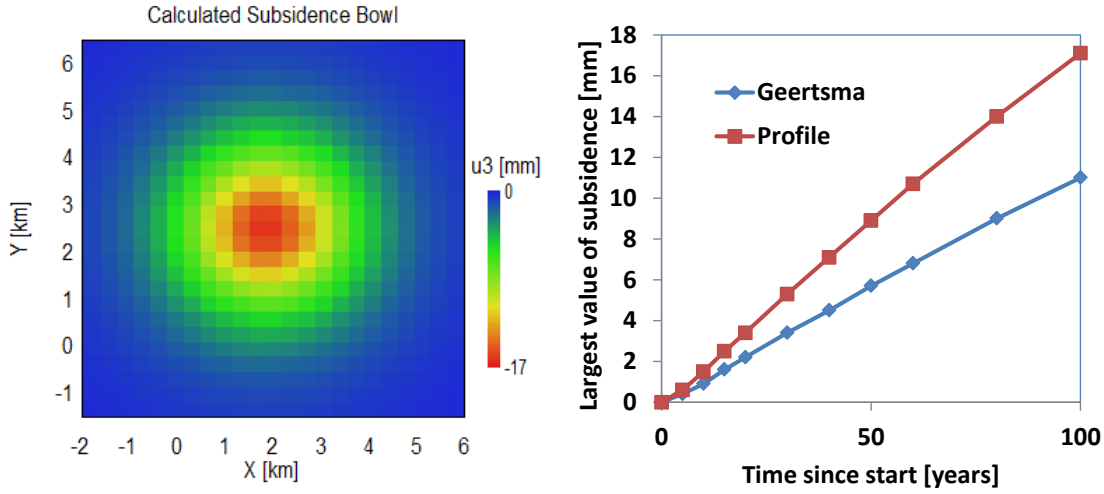

Figure 5 Left: Subsidence profile after 100 years of injection for elastic profile with increasing modulus. Right: temporal development of the deepest value of subsidence for the two cases.

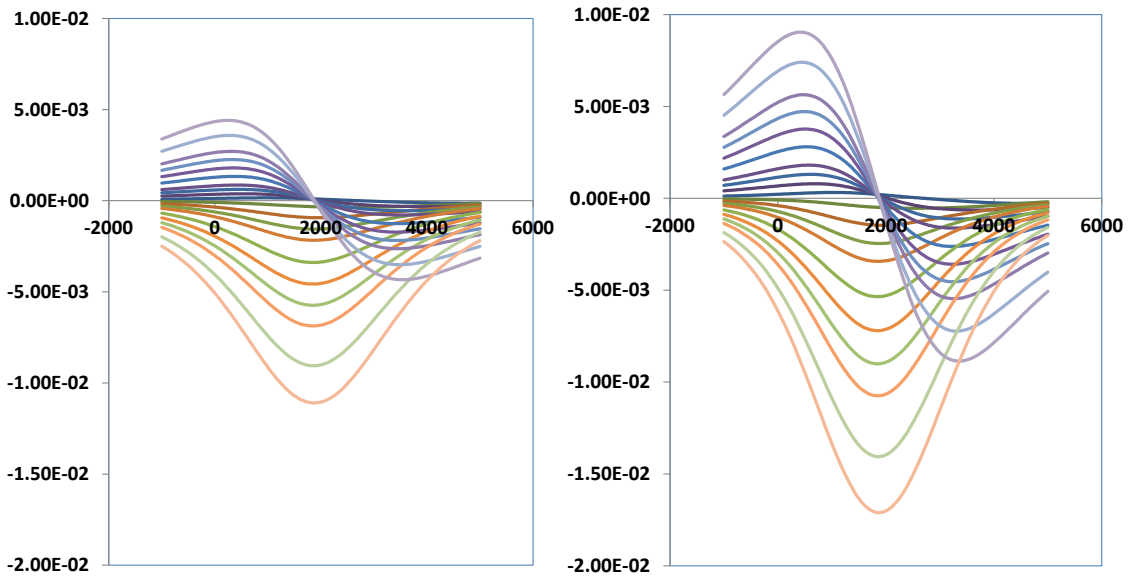

Figure 6 Surface movements along a line above the injection and production well [m] after periods of 5, 10, 15, 20, 30, 40, 50, 60, 80 and 100 years. Blue colors: horizontal movement in the direction of the line (the horizontal movement is toward the centre of the subsidence bowl at the location of the injection well at x = 1750 m). Green / orange lines: Vertical movements. Left: Homogeneous elastic subsurface. Right: Elastic profile according to Fig. 3 (Left). Curves with increasing modulus show larger absolute subsidence values, larger gradients and larger absolute and relative horizontal displacements.

The potential for fault movement is represented as stress paths in Fig. 7. We used a fault with dimensions of 250x500 m and a dip of 70°. The fault was located 300 m from the injection well at the bottom of the reservoir. We found that the influence of distance to the injection well on stress change magnitude is negligible compared to the effect of the distance to the fluid front boundary. It should be noted though that potentially reactivated fault area will be smaller for faults located close to the injection well.

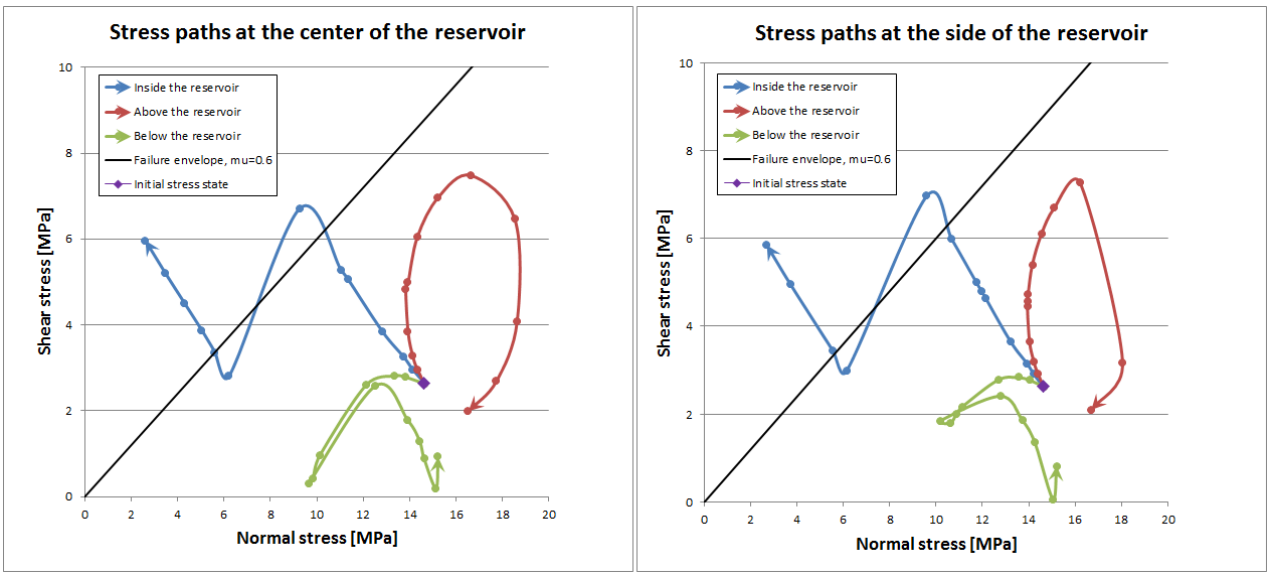

Figure 7 Stress paths for different locations at an example fault of 250x500 m. The stress paths for inside, above and below the reservoir are indicated in blue, red and green, respectively. Left: Stress paths at the center part of the fault. The stress path inside the reservoir is critical and shows that failure will occur when the temperature front passes the fault. No failure occurred for above and below the reservoir. Right: Stress paths at the along-strike side of the fault. Main trends were similar for this location, though small variations due to different orientation with respect to and timing of the temperature front are visible. The data points represent the same time steps for both cases, showing the delay in response for the stress path at the side of the reservoir.

The reservoir as described in the previous section was cross-cut by the fault. This implies an inside-reservoir fault area of 26625 m^2. The thermo-elastic stress change was calculated at grid points inside, below and above the reservoir and converted into a stress path for these points for a passing temperature front. We assumed that the fault was permeable to flow.

Figure 7 shows the stress paths for both in the center of the fault and at the side of the fault. We found that fault activation is restricted to the area inside the temperature front for timescales up to 100 years of injection. The stress path on the fault depended on location in the vertical direction. Inside the reservoir, the stress path was critical and led to failure. A discontinuity appeared when the temperature front passed the fault. Below and above the reservoir, the stress state returned to close-to-initial values and no failure occurred. The deviant shape of the stress path below the reservoir was caused by flipping direction of shear stress vector. Variation in lateral position resulted in small variations in timing and shape of the stress paths. As the temperature front is cylindrical and the fault is a plane feature, the temperature front reached central points at the fault earlier than points at the side (see Fig. 2 right). This led to different timing of the stress paths for varying along-strike points.

We found that for a passing temperature front, the fault will eventually slip over the full areal extent located inside the reservoir. Assuming that slip was indeed restricted to the reservoir as shown in Fig. 7, the area of the fault controls the maximum earthquake magnitude that can occur during cold water injection for geothermal heat production purposes. We used simple seismic relations, which determine the earthquake magnitude based on average stress drop and fault area, to estimate expected earthquake magnitudes. Typical stress drops during induced rupture are in the order of 0.1-10 MPa [e.g. Charléty et al . 2007]. This led to a magnitude range of M=1.4-2.8 for our example fault within the stress drop range. Faults with lateral dimensions smaller than 1000 m are expected to be hard to detect on seismics. For the worst-case scenario with a fault of lateral extent of 1000 m and a maximum stress drop, we obtained a magnitude of M=3.2. As a general rule, onshore shallow seismic events can be felt for M≥2 and can cause damage and seal rupture for M≥3-4 [Nicol et al. 2011]. There is thus a chance that felt events will be produced during geothermal operations, but the risk on damage to the production reservoir is very low.

4. CONCLUDING REMARKS

We have assessed the surface movement and the potential fault activation to be expected from the operation of a geothermal doublet at typical conditions. The largest surface movement is to be expected from the progressive cooling of the reservoir: the cooled area around the injection well grows with time and results in a growing volume of compacted rock, through the thermo-elastic coupling. The absolute value of the expected subsidence is low. The 1 – 2 cm that we model is possibly measureable if circumstances are favourite. In that case the distribution of the subsidence can be used to obtain knowledge about the distribution of the cooled part of the reservoir. In addition, the shape of the subsidence pattern gives information about the subsurface parameters like the elastic profile. Even more important, however, the shape of the subsidence profile will give information about the spatial distribution of the cooled area. This can then be used as an indication for the effectiveness of the doublet and may help when new doublets or wells are planned in the area. The details, however, also depend on the elastic modulus and on the contribution of the pressure inflation and depletion. To unravel this information requires a delicate inversion exercise in which as much information is taken into account as possible (Muntendam-Bos et al, 2008). In particular when horizontal displacements are available alongside vertical displacement, this information can be used in an inversion exercise to constrain the value of the elastic modulus (Fokker et al, 2013). A proper monitoring strategy will help to optimize the information to be obtained (De Waal et al, 2012). We have also shown that the potential for induced fault failure varies with the location on the fault, but the occurrence of failure will most likely be restricted to the reservoir. Associated earthquake magnitudes, based on simple seismic relations, are not expected to cause damage. There is though a small chance that felt events will occur.

REFERENCES

Aki, K.: The upper mantle techtonophysics. *Techtonophysics* **13-1** (1972), p. 423-446.

De Waal, J.A., et al.: The effective subsidence capacity concept: How to assure that subsidence in the Wadden Sea remains within defined limits? *Geologie en Mijnbouw / Netherlands Journal of Geosciences* **91** (2012), 385-399.

Fokker, P.A. and Orlic, B.: Semianalytic modelling of subsidence. *Mathematical Geology* **38** (2006), p. 565-589.

Fokker, P.A., Wassing, B.B.T., Van Leijen, F.J., Hanssen, R.F., and Nieuwland, D.A.: Data Assimilation of PS-InSAR Movement Measurements Applied to the Bergermeer Gas Field. *International Workshop on Geomechanics and Energy*, Lausanne, Switzerland, November 2013.

Geertsma, J.: Land subsidence above compacting oil and gas reservoirs. *Journal of Petroleum Technology* **25** (1973), p. 734-744.

Kramers, L., Van Wees, J.D., Pluymaekers, M., Kronimus, R.A. & Boxem, T. Direct heat resource assessment and subsurface information systems for geothermal aquifers; the Dutch perspective. Netherlands Journal of Geosciences **91-4**, 2012, 637-649.

Muntendam-Bos, A.G., Kroon, I.C., Fokker, P.A.: Time-dependent inversion of surface subsidence due to dynamic reservoir compaction. Mathematical Geosciences, **40** (2008), pp. 159-177

Myklestad, N.O.: Two problems of thermal stress in the infinite solid, *J.Appl.Mech.* **9** (1942), p. 136-143

Nicol, A.; Carne, R. Gerstenbergera, M. Christophersen, A.: Induced seismicity and its implications for CO2 storage risk, *Energy Procedia* **4** (2011), p. 3699–3706

Pluymaekers, M.P.D., Kramers, L., Van Wees, J.-D., Kronimus, A., Nelskamp, S., Boxem, T. & Bonté, D. [2012] Reservoir characterisation of aquifers for direct heat production: Methodology and screening of the potential reservoirs for the Netherlands. Netherlands Journal of Geosciences 91-4, 621-636.

Van Wees, J.D., De Jong, K. and Cloetingh, S.: Two-dimensional P-T-t modelling and the dynamics of extension and compression in the Betic Zone (SE Spain). *Tectonophysics*, **203** (1992): 305-324

Van Wees, J.D., Kronimus, A., Van Putten, M., Pluymaekers, M., Mijnlieff, H., Van Hooff, P., Obdam, A., Kramers, L. Geothermal aquifer performance assessment for direct heat production. Methodology and application to Rotliegend aquifers. Netherlands Journal of Geosciences **91-4**, 2012, 651-665. 54